Korean J. Chem. Eng., 35(11), 2150-2156 (2018)
DOI: 10.1007/s11814-018-0132-7

pISSN: 0256-1115
eISSN: 1975-7220

Optimization of compression ratio in closed-loop CO_2 liquefaction process

Taekyoon Park, Hyungyeol Kwak, Yeonsoo Kim, and Jong Min Lee†

School of Chemical and Biological Engineering, Institute of Chemical Processes, Seoul National University,
1 Gwanak-ro, Gwanak-gu, Seoul 08826, Korea
(*Received 30 April 2018 • accepted 26 July 2018*)

Abstract−We suggest a systematic method for obtaining the optimal compression ratio in the multi-stage closed-loop compression process of carbon dioxide. Instead of adopting the compression ratio of 3 to 4 by convention, we propose a novel approach based on mathematical analysis and simulation. The mathematical analysis prescribes that the geometric mean is a better initial value than the existing empirical value in identifying the optimal compression ratio. In addition, the optimization problem considers the initial installation cost as well as the energy required for the operation. We find that it is best to use the fifth stage in the general closed-loop type carbon dioxide multi-stage compression process.

Keywords: Carbon Capture, Closed-loop Compression, Compression Ratio, Multi-stage Compression, Geometric Mean

INTRODUCTION

A liquefaction process is essential to capture, store, and utilize carbon dioxide from various sources. Carbon dioxide is re-liquefied by a multi-stage compression process for transport through pipelines or using ships. In this case, the number of compressors and the compression ratio in each compressor serve as the decision variables for the initial investment and operation cost of the entire process, as well as the process configuration.

Heuristics are widely used to determine the number of compressors and the compression ratio [1-3]; however further optimization is still required in each process to improve performance and economy. Based on the simulation, various alternatives to the compression process for ship transport are reviewed and additional energy and cost are reduced through additional compression ratio optimization [4]. Similarly, through simulations, more design variables are included to improve the separation efficiency compared to existing process [5]. On the other hand, optimization studies have been carried out on a new process of subdividing a dehydration process [6]. In addition, temperature change of seawater, a new variable not considered in the previous studies, is considered to optimize a re-liquefaction process [7]. However, there is a fundamental limit to the optimization that focuses only on the compression process, because the optimal condition obtained from the compression process can be changed in terms of the entire process.

Beyond the compression process, optimization studies have been conducted from the viewpoint of the whole process. Aspelund et al. [8] report the energy, exergy, and cost of carbon dioxide processing through ship transportation from the perspective of the entire process. In addition, optimization of an entire process including a compression process focusing on separation process is proposed [9]. However, process design and optimization considering all possible cases are impossible, and optimization from the perspective of the whole process involves simplified representation of compression process.

Some studies suggest a new method from the viewpoint of searching for the optimal compression ratio rather than based on a specific process. Although there is a limitation on ship transportation, the intermediate pressure optimization with the same discharge temperature (IPODT) method has been proposed for selecting the optimal compression ratio, rather than using a heuristic method or simulation based intermediate pressure optimization (IPO) method [10]. In addition, the impacts of various types of compressors are investigated and setting optimal compression ratios is considered for each case [11].

However, most studies to date are based on simulations and focus on yielding quantitative results rather than qualitative explanations, that is, simply providing better results than those in the past proposed process without rationales. This methodology is consequently included in the framework of process modeling, time-consuming simulation, and best result selection. In this study, we looked at the optimal compression ratio decision problem in both qualitative and quantitative perspectives, rather than a somewhat 'simulation-and-selection' approach. First, the optimal compression ratio was mathematically determined from a well-known equation. Simulation using MATLAB and PRO/II was performed to discuss the difference between the two results. Based on the results, we proposed a process of setting the initial values for the optimal solution search in a general multistage compression process.

PROBLEM FORMULATION

1. Energy Required for CO_2 Liquefaction

Thermodynamic analysis of liquefaction and cooling process is convenient with P-H-line (Pressure-enthalpy diagram) which presents the enthalpy on the abscissa and the pressure on the ordinate. Fig. 1 represents the closed-loop carbon dioxide liquefaction process on the P-H diagram. Because the compression ratio of a com-

†To whom correspondence should be addressed.
E-mail: jongmin@snu.ac.kr

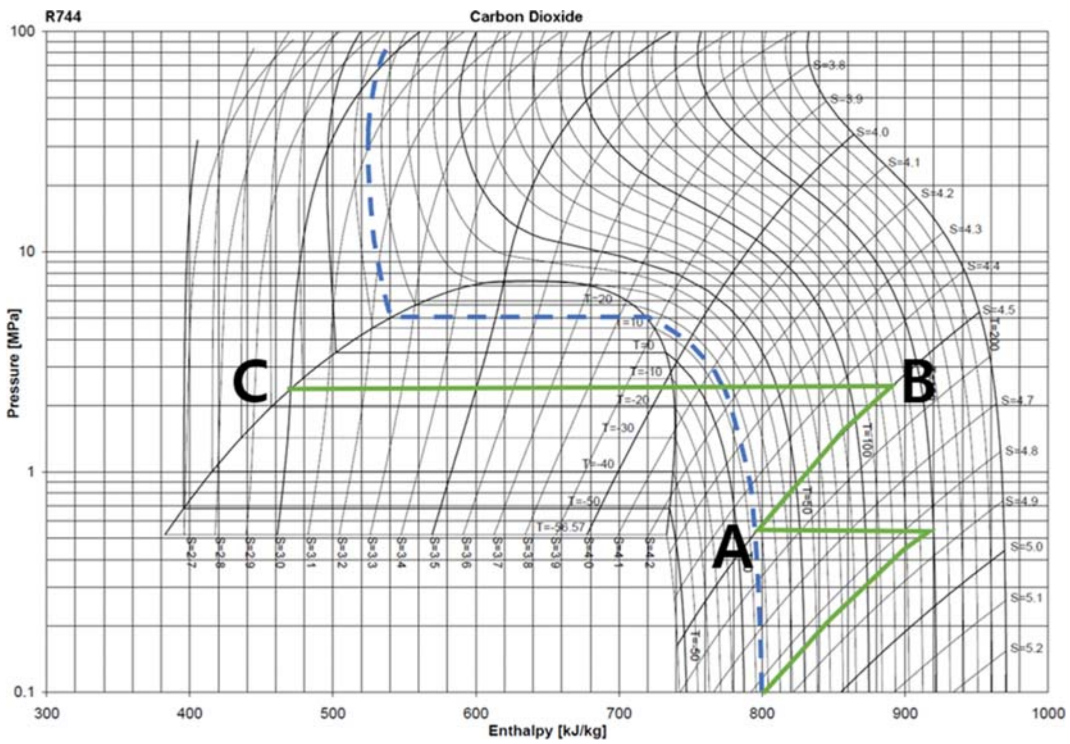

Fig. 1. P-H diagram of closed-loop carbon dioxide liquefaction process [7].

pressor is physically constrained, it is impossible to obtain the final pressure with only one compressor; thus, multi-stage compressors are usually required. The dotted line represents a constant isothermal line with the temperature of 15 °C, which is the result of assuming the cooling water temperature of 10 °C and minimum approach temperature of 5 °C. The segment AB is the isentropic line with a constant entropy. The segment BC represents a process of cooling the pressurized stream with cooling water and refrigerant to the final pressure. This is an isobaric process assuming that there is no pressure drop between the units of operation. Hence, it is represented by a horizontal line. The point C can be liquefied with carbon dioxide by lowering the temperature to the dew point at the corresponding pressure. Under an adiabatic process with negligible changes in kinetic and potential energy, the compression work is given by

$$W=\Delta H=H_2-H_1 \tag{1}$$

That is, the compression work required is equal to the difference in the enthalpy values corresponding to A and B in Fig. 1.

If we define the heat capacity ratio for ideal gas, the constant volume heat capacity C_v can be expressed with k and the gas constant R as in Eq. (2).

$$k\equiv\frac{C_p}{C_v}=\frac{C_v+R}{C_v}=1+\frac{R}{C_v},\ C_v=\frac{R}{k-1} \tag{2}$$

Since the compressor operates adiabatically, W of the continuous adiabatic compression process can be derived as

$$\begin{aligned} W &= \mu C_p \Delta T=\mu k\frac{R(T_2-T_1)}{k-1}=\mu k\frac{p_2V_2-p_1V_1}{k-1} \\ &= \frac{\mu k p_1 V_1}{k-1}\left[\left(\frac{p_2}{p_1}\right)^{\frac{k-1}{k}}-1\right]=\frac{\mu k R T_1}{k-1}\left[\left(\frac{p_2}{p_1}\right)^{\frac{k-1}{k}}-1\right], \end{aligned} \tag{3}$$

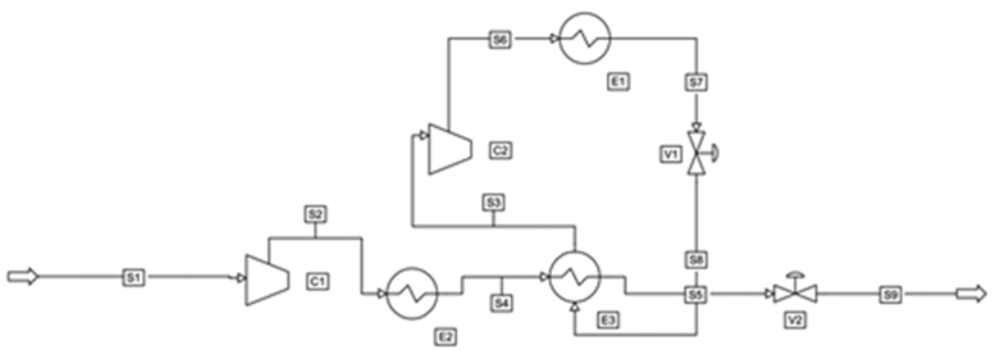

Fig. 2. Process flow diagram of closed-loop liquefaction process.

where μ is the molar flow rate. If the compression stage is composed of multiple stages, the intercooler and the flash drum are installed so that the liquefied moisture is removed. The total compression rate W can be expressed as

$$\begin{aligned} W &= W_1 + W_2 + W_3 + \cdots + W_i \\ &= \frac{kRT}{k-1}\left[\mu_1\left(\frac{P_2}{P_1}\right)^{\frac{k-1}{k}} + \mu_2\left(\frac{P_3}{P_2}\right)^{\frac{k-1}{k}} + \mu_3\left(\frac{P_4}{P_3}\right)^{\frac{k-1}{k}} + \cdots \right. \\ &\quad \left. + \mu_i\left(\frac{P_{i+1}}{P_i}\right)^{\frac{k-1}{k}} - (\mu_1 + \mu_2 + \mu_3 + \cdots + \mu_i)\right], \end{aligned} \tag{4}$$

and Fig. 2 shows a process flow diagram of the typical closed-loop liquefaction process.

2. Constraints

Composition, pressure, and temperature of the carbon dioxide stream from the CO_2 capture process using monoethanolamine (MEA) were used as the conditions of the influent. Originally, the emissions from the capture process are mixed with trace amounts of MEA, unburned fuel, and by-products of the combustion process. Since these are included in very small amounts, we assume that the influent gas is simply a mixture of carbon dioxide and water vapor. The water content in the product should be less than 500 ppm to prevent solid hydrate formation. The final temperature is the temperature at which the pressurized carbon dioxide becomes a saturated liquid. The input and output conditions are summarized in Table 1.

In the case of pressure, the minimum value is the inflow pressure and the maximum value is the final pressure. To determine the final pressure, we examined the molar fraction of water present in the meteorological conditions with different pressures. The temperature was determined as 15 °C because the intercooler temperature was assumed to be 10 °C and the minimum approach temperature was assumed to be 5 °C. The molar fraction of water in the gas phase according to the pressure obtained from the case study is shown in Fig. 3.

The ordinate of the plot is in the log scale. It can be seen that the mole fraction of the gas side decreases with increasing pressure, because the larger the pressure, the greater the amount of water exiting into the liquid phase. In addition, at a specific pressure (56.7 bar), the molar fraction of water is minimized and then rapidly increased again, depending on the phase change of the mixture at this pressure. That is, as some portion of the gaseous carbon dioxide is liquefied, the water fraction in the vapor phase increases sharply. Therefore, pressurizing above 56.7 bar does not help to remove moisture from the gas phase. The minimum compression ratio was set to 2 considering economic efficiency. The maximum value was determined to be 4 according to the rule of thumb used in practice. If the lower and upper bounds of the compression ratio are held in this way, the number of compression stages is also determined from the pressure constraints. Since the pressure is increased from 1 bar to 56.7 bar, considering the range of general compression ratio, the number of compression stages is preferably between 3 and 5 [12].

Table 1. Input and output constraints

	Feed	Product
Temperature (°C)	45	Temperature of the saturated liquid (at final pressure)
Pressure (bar)	1	56.7
Flowrate (kg/hr)	323,406 kg/hr (7562.81 kg-mol/hr)	N/A (Dependent variable)
Composition (mole fraction)	CO_2 0.9520 H_2O 0.0480	H_2O<500 ppm

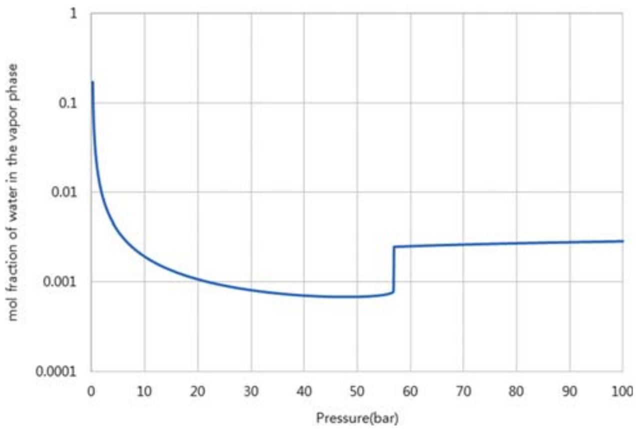

Fig. 3. Molar fraction of water according to the pressure.

RESULTS

1. Mathematical Approach

1-1. n=2

If there are two compressors, the total energy requirement can be expressed by

$$\begin{aligned} W &= \frac{kRT}{k-1}\left[\mu_1\left(\frac{P_2}{P_1}\right)^{\frac{k-1}{k}} + \mu_2\left(\frac{P_3}{P_2}\right)^{\frac{k-1}{k}} - (\mu_1+\mu_2)\right] \\ &= \frac{kRT}{k-1}\left[\mu_1\left(\frac{P_2}{1}\right)^{\frac{k-1}{k}} + \mu_2\left(\frac{56.7}{P_2}\right)^{\frac{k-1}{k}} - (\mu_1+\mu_2)\right] \\ &= A[\mu_1(r_1^{\gamma}-1) + \mu_1\{1-B(1-r_1^{\delta})\}(r_2^{\gamma}-1)] \\ &= A\mu_1[(r_1^{\gamma}-1) + \{1-B(1-r_1^{\delta})\}(r_2^{\gamma}-1)] \\ &\left(r_1 = \frac{P_2}{1},\ r_2 = \frac{56.7}{P_2},\ \gamma = \frac{k-1}{k}\right). \end{aligned} \tag{5}$$

B is a constant obtained from the regression between pressure and mole fraction of water, and its value is 0.01153. For the convenience of calculation, the objective function J can be expressed in a simpler form: The heat capacity ratio k was also treated as a constant in this process. Although the heat capacity ratio is affected by temperature and density, we assumed that dependence on the temperature and density is negligible. In Eq. (5), the rest of the parameters excluding the constants in front of the square brackets are set as objective functions (see Eq. (6)).

$$J = r_1^{\gamma} + r_2^{\gamma} + B\{r_1^{\delta} r_2^{\gamma} - (r_1^{\delta} + r_2^{\gamma})\} \tag{6}$$

To examine the optimal solution by a sequential method instead of a simultaneous method, the objective function J is divided into two parts, J_1 and J_2.

$$J_1 = r_1^{\gamma} + r_2^{\gamma},\ J_2 = B\{r_1^{\delta} r_2^{\gamma} - (r_1^{\delta} + r_2^{\gamma})\}. \tag{7}$$

In the case of n=2, since the decision variable is solely p_1, the changes of J_1 and J_2 were examined according to p_1.

In the case of J_1, the product of r_1 and r_2 is constant, which is a typical optimization problem. The situation where r_1 and r_2 are equal to the value of the geometric mean becomes optimal. In the case of J_2, the term $(r_1^{\delta} r_2^{\gamma})$ is always smaller than or equal to the summation term $(r_1^{\delta} + r_2^{\gamma})$, and it is easy to observe that J_2 approaches 0 as p_1 increases; however, the minimum value is hardly identifiable. Fig. 4 shows that the minimum value of J_2 occurs near p_1=4. J, the sum of J_1 and J_2, has its optimal value near p_1=7.4, which is about 1.8% smaller than the geometric mean of 7.529. This is because the point where $\frac{dJ_1}{dp_1} + \frac{dJ_2}{dp_1} = 0$ occurs at p* which is smaller than p_1= 7.529 where minimum of J_1 occurs. From the numerical observation, the compression ratio that minimizes the energy required for n=2 is located in a range smaller than the geometric mean, and the difference is expected to be insignificant. The geometric mean therefore serves as a good initial value.

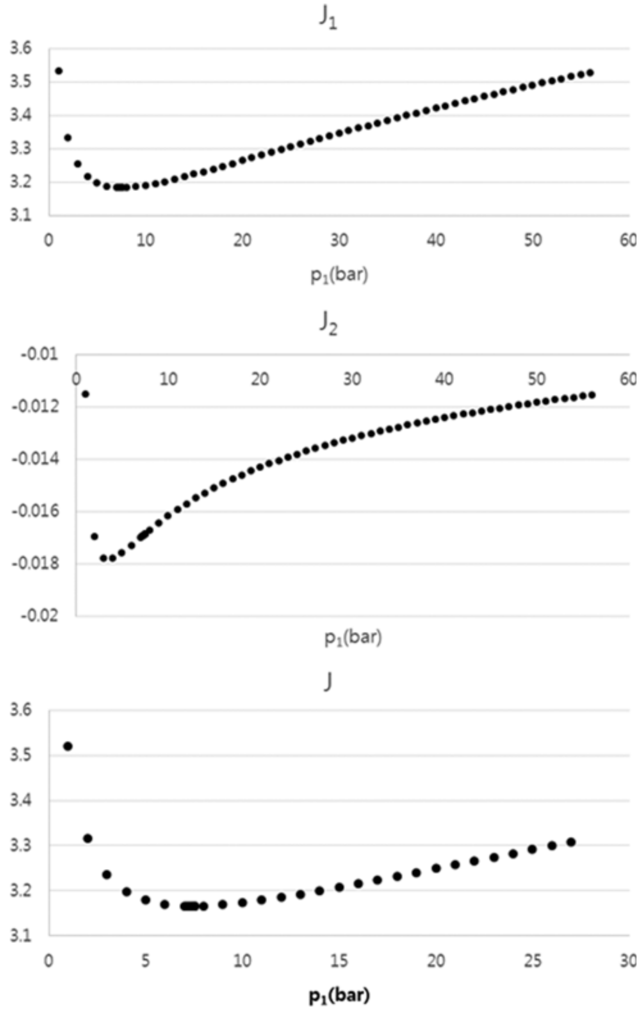

Fig. 4. J_1, J_2 and J according to p_1.

1-2. n≥3

The general case can be expressed as

$$J = f(r_i) + Bg(r_i). \tag{8}$$

For n=k, J has (k−1) decision variables, r_i (i=1, 2, …, k−1). $f(r_i)$ represents Σr_i^{γ} and it has an optimal solution when r_i is constant (geometric mean, G.M.) for all i=1, 2, …, k−1. $Bg(r_i)$ is always smaller than 0 and its optimal solution is located in the interval of r_i<G.M. for all i=1, 2, …, k−1. In addition, it approaches 0 as r_i increases to its maximum value. As a result, each component of the optimal solution vector of J has a value smaller than G.M., which is a better initial value than the heuristic ratio of 3-4. This interpretation is valid only if k in the exponent of the objective function (in γ) is independent of temperature and pressure.

2. Simulation-based Approach

In general, it is assumed that there is no pressure drop in each unit in order to facilitate the optimization process through computation, although the steam pressure decreases through the process units. The temperature of the stream passing through the intercooler was fixed at 15 °C to remove the effect of temperature change. The compressor was assumed to pressurize through isentropic process, and adiabatic condition without heat input was specified for the flash. Finally, for the convenience of calculation, the adiabatic efficiency was assumed to be 100%.

Economics can be divided into two parts: operating cost and equipment installation cost. In case of carbon dioxide liquefaction process, operation cost may include electricity cost for running compressor, cost for cooling water, maintenance cost for refrigerant, etc. Installation cost is incurred for the compressor, heat exchanger, flash drum, and valve. We focused on the compressor only, because it occupies the largest portion of the total cost of the liquefaction process. The operation cost is for the electricity of the compressor, and the installation cost is for the procurement and installation of the compressor. Electricity cost was specified as \$ 0.065/kWh based on the 2010 report of the US Department of Energy. The following relation was used to estimate the installation cost of the compressor [14]. The number in the equation is the ratio of the Chemical Engineering Plant Cost Index (CEPCI). This formula is based on 1968 and the value is updated according to the latest published price index [15].

$$\text{Installation Cost (\$)} = \frac{558.3}{119} \times 515.7(\text{bhp})^{0.82}(2.11 + F_c) \tag{9}$$

(1 kW=1.3410 bhp, F_c=1 for centrifugal motor type).

The operating cost is annual, whereas the installation cost is spent only once, and the installation cost must be annualized in order to combine the two costs. For this purpose, we divided the installation cost by the payback period and used the total annual cost (TAC) combined with the operation cost as the objective function to minimize.

Table 2. Simulation result obtained from MATLAB (OPEX)

Number of stages	P_{r1}	P_{r2}	P_{r3}	P_{r4}	P_{r5}	W (kW)
3	3.794	3.854	3.877	-	-	22953.79
4	2.714	2.743	2.756	2.763	-	22028.04
5	2.221	2.238	2.247	2.252	2.254	21496.16

$$\text{Total annual cost (TAC)} = \frac{\text{Installation cost}}{\text{payback period}} + \text{operating cost.} \quad (10)$$

2-1. Required Energy

2-1-1. MATLAB

Table 2 shows the optimized compression ratio, pressure, and total power consumption calculated from MATLAB. The shaded value is not an independent variable, and it is the value calculated from the optimized value and the determined final pressure. The minimum total power consumption is 21496.16 kW, which is the lowest power among the three cases.

2-1-2. PRO/II

Table 3 shows the optimization results using the PRO/II optimizer. The compression ratio is quite different from that of MATLAB. This is because the heat capacity ratio k of 1.3 is not a constant but a temperature dependent variable. In the process flowsheet simulator, Pro/II, these temperature-dependent variables are calculated and reflected in the calculation process. As for the total power requirement, we found that case with five stages is the minimum with 20153.9 kW like the result of MATLAB.

2-2. Economic Evaluation

2-2-1. MATLAB

As a result of the economics analysis based on the optimization result of MATLAB, the operating cost showed a tendency to decrease as the number of stages increased because of the proportion of the total power consumption. However, the annualized installation cost increased as the number of stages increased. The TAC was the most economical at \$27.452 M/yr at stages 4 and 5.

2-2-2. PRO/II

Unlike MATLAB, TAC was the most economical at \$25.87 M/yr for stage 5 since the heat capacity ratio is considered as a variable in simulation using PRO/II.

Table 3. Simulation result obtained from Pro/II (OPEX)

Number of stages	P_{r1}	P_{r2}	P_{r3}	P_{r4}	P_{r5}	W (kW)
3	4	4	3.543	-	-	21824.3
4	2.904	2.916	2.790	2.399	-	20773.7
5	2.350	2.363	2.368	2.236	1.926	20153.9

Table 4. Simulation result obtained from MATLAB (OPEX+CAPEX)

Number of stages	Total installation cost (M\$)	Operating cost (M\$/yr)	Annualized installation cost (M\$/yr)	TAC (M\$/yr)
3	43.929	13.069	14.643	27.712
4	44.728	12.542	14.909	27.452
5	45.637	12.239	15.212	27.452

Table 5. Simulation result obtained from Pro/II (OPEX+CAPEX)

Number of stages	Total installation cost (M\$)	Operating cost (M\$/yr)	Annualized installation cost (M\$/yr)	TAC (M\$/yr)
3	42.123	12.426	14.041	26.467
4	42.560	11.828	14.186	26.015
5	43.189	11.475	14.396	25.872

Table 6. Optimal compression ratio for each case (vs. G.M.)

n	vs G.M.	P_r (Mathematical)	P_{r1}	P_{r2}	P_{r3}	P_{r4}	P_{r5}
3	3.841		4	4	3.5437	-	-
	Ratio		1.041	1.041	0.922	-	-
4	2.744	r_1<G.M.	2.9043	2.916	2.790	2.399	-
	Ratio		1.058	1.062	1.016	0.874	-
5	2.242		2.35	2.363	2.368	2.236	1.926
	Ratio		1.047	1.054	1.056	0.997	0.859

3. Comparison

The comparison between mathematical optimization and simulation results using PRO/II is shown in Table 6.

The compression ratio was greater than the geometric mean, except for the last one or two compressors. This was different from the result of the mathematical optimization that the compression ratio must be smaller than the geometric mean. These errors are due to the following reasons: First, as the actual multi-stage compression progresses, phase separation occurs and the compression efficiency decreases. Therefore, it is advantageous to use a high compression ratio at the beginning in terms of the total energy. Second, the temperature and pressure change, and thus the heat capacity ratio, which was treated as a constant in the mathematical optimization, changes.

As a result, we can summarize the optimal compression ratio in the closed-loop CO_2 multistage compression process as follows.

(1) Geometric averages are good candidates at the beginning of optimization.

(2) To obtain faster convergence, it is better to set a value smaller than the geometric mean for the first and second stages and a value larger than the geometric mean for the remaining multi-stage compression.

(3) The heat capacity ratio depends on the temperature and the density, and the temperature and density changes occurring during the compression process cannot be completely ignored in obtaining an optimum compression ratio in practice.

(4) As the temperature increases, the heat capacity ratio increases and $\frac{k-1}{k}$ in the exponent position increases, which affects the optimal compression ratio. However, the effect gradually decreases because it is a fractional function form. This applies to the compression ratios of the remaining stages except for the last compression stage being slightly larger than or similar to the geometric mean.

CONCLUSION

We optimized the compression ratio in CO_2 liquefaction process to make it an energy efficient and economical process for transporting CO_2 capture and storage (CCS). The optimization was carried out in two ways: mathematical optimization and simulation-based optimization. When the heat capacity ratio was treated as a constant, the use of a compression ratio smaller than the geometric mean was most advantageous in terms of OPEX. When the heat capacity ratio was treated as a variable depending on the temperature in the simulation using Pro/II, the optimum compression ratio as well as the optimum number of stages were different from the geometric mean. In this case, it is best to use a compression ratio that is about 4-5% higher than the geometric average in the remaining stages except for the last stage. For the last stage, we recommended a compression ratio lower than the geometric mean. This was because as the compression ratio increased, the temperature of the mixture of carbon dioxide and water increased, and thus there existed a tradeoff due to the increase in the term $\frac{k-1}{k}$ of the exponent. As with mathematical methods, MATLAB simulation results with the constant heat capacity ratio showed similar results with mathematical optimization. In the simulation with Pro/II, it was found to be more economical to use a compression ratio higher than the geometric mean at the beginning of multi-stage compression. Considering OPEX alone and considering both OPEX and CAPEX, the five-stage multi-stage compression process was more economical than the three or four-stage multi-stage compression. Based on these results, we could summarize the optimal compression ratio search procedure for the closed-loop type multi-stage compression process as follows.

(1) Find possible numbers of compressors for a multi-stage compression using ratio of 3 to 5.

(2) Set the compression ratio excluding the last two stages to be higher than the geometric average.

(3) Proceed with numerical optimization.

(4) Compare the results of the process using different compressor numbers.

ACKNOWLEDGEMENTS

This work was supported by the National Research Foundation of Korea (NRF) Grant funded by the Korean Government (MSIT) [NRF-2016R1A5A1009592] and by Engineering Development Research Center (EDRC) funded by the Ministry of Trade, Industry & Energy (MOTIE) [No. N0000990].

NOMENCLATURE

W : compression work
H : enthalpy
C_p : the constant pressure heat capacity
C_v : the constant volume heat capacity
R : the gas constant
k : heat capacity ratio
μ : molar flow rate
T : temperature
p : pressure
V : volume
J : objective function
A : constant equal to $\frac{kRT}{k-1}$
B : constant equal to 0.01153
n : number of stages

REFERENCES

1. W. D. Seider, J. D. Seader, D. R. Lewin and S. Widagdo, Product and process design principles: Synthesis, analysis and design, Wiley, 3rd Ed. (2008).
2. N. V. S. N. Murthy Konda, G. P. Rangaiah and D. K. H. Lim, *Ind. Eng. Chem. Res.*, **45**(17), 5955 (2006).
3. W. L. Luyben, *Ind. Eng. Chem. Res.*, **50**(24), 13984 (2011).
4. U. Lee, S. Yang, Y. S. Jeong, Y. Lim, C. S. Lee and C. Han, *Ind. Eng. Chem. Res.*, **51**(46), 15122 (2012).
5. S. Posch and M. Haider, *Fuel*, **101**, 254 (2012).

6. K. T. Leperi, R. Q. Snurr and F. You, *Ind. Eng. Chem. Res.*, **55**(12), 3338 (2016).
7. S. G. Lee, G. B. Choi and J. M. Lee, *Ind. Eng. Chem. Res.*, **54**(51), 12855 (2015).
8. A. Aspelund, M. J. Mølnvik and G. D. Koeijer, *Chem. Eng. Res. Design*, **84**(9), 847 (2006).
9. T. Park, S. G. Lee, S. H. Kim, U. Lee, C. Han and J. M. Lee, *Int. J. Greenhouse Gas Control*, **46**, 271 (2016).
10. S. H. Jeon and M. S. Kim, *Appl. Therm. Eng.*, **82**, 360 (2015).
11. J. Kotowicz, M. Brzęczek and M. Job, *Int. J. Global Warming*, **12**(2), 164 (2017).
12. J. Moore and M. G. Nored, *ASME Turbo Expo: Power for Land, Sea, and Air*, **7**, 645 (2008).
13. M. Moshfeghian, Variation of Ideal Gas Heat Capacity Ratio with Temperature and Relative Density (Tip of the Month), John M. Campbell & Co., Norman, OK, U.S.A. (2013).
14. J. M. Douglas, Conceptual Design of Chemical Processes, McGraw-Hill (1988).
15. CEPCI June 2017 Issue, SCRIBD, https://www.scribd.com/document/352561651/CEPCI-June2017-Issue, Accessed 11 Dec. 2017.